Research Square

Preprints are preliminary reports that have not undergone peer review.
They should not be considered conclusive, used to inform clinical practice,
or referenced by the media as validated information.

Beyond the Metal Core: In Silico Safety Profiling of the Capping Phytoconstituents of Oxystelma esculentum Ag/AgCl Nanoparticles for Cardiac, Endocrine and Cytochrome P450 Risk

Muhammad Akhlaq

muhammadakhlaq377@gmail.com

Hamdard University https://orcid.org/0000-0001-6821-4193

Research Article

Keywords: Oxystelma esculentum, green synthesis, capping phytoconstituents, safety profiling, hERG, cytochrome P450, endocrine disruption, toxicity prediction

Posted Date: November 16th, 2026

DOI: https://doi.org/10.21203/rs.3.rs-11727139/v1

License: This work is licensed under a Creative Commons Attribution 4.0 International License.
Read Full License

Additional Declarations: The authors declare no competing interests.

Beyond the Metal Core: In Silico Safety Profiling of the Capping Phytoconstituents of Oxystelma esculentum Ag/AgCl Nanoparticles for Cardiac, Endocrine and Cytochrome P450 Risk

Muhammad Akhlaq[1*]

[1]Office of Research, Innovation and Commercialization (ORIC), Hamdard University Karachi, Pakistan

* for correspondence :muhammadakhlaq377@gmail.com

Abstract

Green-synthesised silver/silver chloride (Ag/AgCl) nanoparticles carry a surface layer of the plant constituents that reduce and cap them, and that capping layer is part of what a biological system meets. We profiled the safety-related behaviour of twelve capping phytoconstituents of Oxystelma esculentum Ag/AgCl nanoparticles epicatechin, kaempferol, lupeol, stigmasterol, esculin, chlorogenic acid, gallic acid, 4-hydroxybenzoic acid, caffeic acid, ferulic acid and coumarin, with silybin as a reference standard across five computational work packages: physicochemical and drug-likeness descriptors, structural-alert screening, toxicity prediction with two independent predictors, docking against a cardiac, endocrine and cytochrome P450 panel, and a reasoned safety synthesis. No constituent was predicted hepatotoxic by ProTox 3.0, and none was predicted mutagenic by the same predictor, but the predictors disagreed on mutagenicity for three constituents and on hepatotoxicity for one, and both disagreements are reported rather than resolved by fiat. Three constituents lupeol, stigmasterol and silybin combined the strongest predicted hERG pore-site binding (−9.09, −7.94 and −8.93 kcal/mol) with positive hERG II predictions, a qualitative agreement that marks them for experimental cardiac follow-up. Coumarin carried the strongest acute-toxicity signal (predicted LD50 196 mg/kg, the only GHS Class 3 value). Lupeol was the most selective binder in the panel: the strongest at CYP3A4 (−10.50 kcal/mol) and hERG yet a non-binder at the androgen receptor, CYP2D6 and CYP1A2. Silybin, the strongest oestrogen-receptor-α binder (−9.29 kcal/mol), was a non-binder at the androgen receptor and CYP1A2 and carried the only predicted cardiotoxicity flag. All findings are predictions, not experimental toxicity data. Two 10 ns molecular dynamics runs support the docked endocrine poses: silybin remained bound in oestrogen receptor α (mean 1.70 protein–ligand hydrogen bonds per frame, anchored at Glu353 in 96% of frames) and epicatechin remained bound in the androgen receptor (mean 2.26 hydrogen bonds per frame, anchored at Thr877 in 53% of frames), with ligand root-mean-square deviation of 0.18 and 0.16 nm after protein fitting.

Keywords: Oxystelma esculentum; green synthesis; capping phytoconstituents; safety profiling; hERG; cytochrome P450; endocrine disruption; toxicity prediction

1. Introduction

Plant-mediated (green) synthesis has become a widely used route to silver nanoparticles because the plant extract serves simultaneously as reductant and stabiliser, avoiding hazardous reagents and yielding particles whose surfaces carry adsorbed phytochemicals. Those adsorbed constituents the capping layer are not inert packaging: they determine colloidal behaviour, they are presented to cells alongside the metal core, and, as the particle degrades or the layer desorbs, they may act as free compounds in their own right. A safety assessment of a green-synthesised nanoparticle that ignores its capping layer is therefore incomplete.

Oxystelma esculentum (L. f.) Sm. (Apocynaceae) is a medicinal climbing plant of the Cholistan Desert and Indus plains whose leaves and latex are used traditionally for urinary, febrile and hepatic complaints. We have previously reported O. esculentum-mediated Ag/AgCl nanoparticles with potent concentration-dependent antineoplastic activity against MCF-7, HeLa and HepG2 cells (IC50 1.10 ± 0.04, 0.90 ± 0.03 and 0.90 ± 0.03 μg/mL) [1], and a hydroalcoholic extract of the same plant with cytotoxic activity against human cancer cell lines [2]. The ethanolic extract of O. esculentum has also been characterised in vivo, with anti-inflammatory, analgesic and antipyretic activity at 100–500 mg/kg and a phenolic profile determined by high-performance liquid chromatography (HPLC) [3]. That HPLC profile identified six phenolics chlorogenic acid, gallic acid, 4-hydroxybenzoic acid, caffeic acid, ferulic acid and coumarin and our earlier experimental programme isolated five further constituents from the leaf extract: epicatechin, kaempferol, lupeol, stigmasterol and esculin. Together with silybin, included as a hepatoprotective reference standard, these twelve compounds form the panel assessed here.

The safety questions that matter first for such a panel are practical ones. Do any constituents carry structural features associated with assay interference or reactive toxicity? Do predictors flag organ toxicity, mutagenicity or carcinogenicity? Do they bind the cardiac hERG potassium channel, whose blockade is a leading cause of drug withdrawal? Do they engage the major drug-metabolising cytochrome P450 enzymes, implying drug–drug interaction potential? And do they engage the oestrogen and androgen receptors, implying endocrine activity? We addressed these questions computationally, in five work packages, because computational profiling can prioritise the small number of constituents and endpoints that most deserve scarce experimental capacity and because every prediction reported here is explicitly labelled as a prediction, with disagreements between predictors preserved rather than smoothed over.

This manuscript is deliberately a safety study, not an efficacy study. Binding scores are reported as predicted affinities for prioritisation; they are not measurements of inhibition, activation or toxicity, and no constituent is described as toxic or safe on the basis of these calculations alone. Section 2 describes the methods and their qualifications in full, including three failed or limited procedures that constrain what can be claimed. Section 3 reports each work package, Section 4 synthesises a prioritised safety ranking, and Section 5 states the limitations that bound every conclusion.

2. Methods

2.1. Compound panel

The panel comprised the twelve compounds listed in Table 1. Structures were taken from PubChem [13] by compound identifier (CID) and used as the SMILES strings given in the deposit pack. Silybin was included as a reference standard because of its established hepatoprotective use, not because it is a constituent of the extract; all other panel members are constituents of, or identified in, the O. esculentum leaf extract as described above.

Compound	PubChem CID	Molecular formula
Epicatechin	72276	C15H14O6
Kaempferol	5280863	C15H10O6
Lupeol	259846	C30H50O
Stigmasterol	5280794	C29H48O
Esculin	5281417	C15H16O9
Chlorogenic acid	1794427	C16H18O9
Gallic acid	370	C7H6O5
4 Hydroxybenzoic acid	135	C7H6O3
Caffeic acid	689043	C9H8O4
Ferulic acid	445858	C10H10O4
Coumarin	323	C9H6O2
Silybin	31553	C25H22O10

Table 1. The twelve-compound panel. Formulae computed from the panel SMILES strings; CIDs as used for structure retrieval.

2.2. WP1 — Physicochemical descriptors and drug-likeness

Descriptors were computed locally with RDKit [14]: molecular weight (MW), Crippen logP, topological polar surface area (TPSA), hydrogen-bond donors (HBD) and acceptors (HBA), and rotatable-bond count (RotB). Lipinski violations [10] and Veber pass/fail [11] (TPSA ≤ 140 Å² and RotB ≤ 10) were recorded per compound. RDKit values are reported as primary; SwissADME values (Section 2.4) are a cross-check, not merged with them, because the two tools use different logP models.

2.3. WP2 — Structural-alert screening

Pan-assay interference (PAINS) [8] and Brenk [9] alerts were assigned with the RDKit FilterCatalog, reported catalogue-separated. These alerts flag substructures historically associated with assay interference or reactive behaviour; they are screening flags, not toxicity verdicts, and Section 3.3 states this explicitly for the catechol flags found here.

2.4. WP3 — Toxicity and ADME prediction

Three web predictors were attempted on 25 October 2026; one failed and is reported as such. SwissADME (swissadme.ch) was run as a single twelve-compound batch and used as a cross-check for

drug-likeness, gastrointestinal (GI) absorption, blood–brain barrier (BBB) permeation, solubility and lipophilicity [5]. ProTox 3.0 (tox.charite.de/protox3) was used for acute oral toxicity (predicted LD50 and GHS class), hepatotoxicity, neurotoxicity, nephrotoxicity, cardiotoxicity, carcinogenicity, immunotoxicity, mutagenicity (labelled "Mutagenicity" on the site; the Ames endpoint), Tox21 nuclear-receptor flags and molecular initiating events (MIE), with "All" additional models selected [6]. One qualification must accompany every ProTox value in this manuscript: the ProTox input page provides no file-upload control, so these runs were not SMILES-typed; each ligand was entered through the site's own PubChem-name search, which displayed "Selected molecule: [ligand name]" before prediction, and the structure resolved by PubChem name was used. pkCSM (biosig.lab.uq.edu.au/pkcsm) was used for AMES toxicity, hERG I and hERG II inhibition, hepatotoxicity, skin sensitisation, LD50, lowest observed adverse effect level (LOAEL) and maximum tolerated dose [7]. Two qualifications apply. First, pkCSM was run one compound at a time in single-molecule mode because its batch mode rejected the input file for missing column headers. Second, lupeol was run on a connectivity-only SMILES because the site rejected the stereochemical SMILES twice; the site-reported molecular weight (426.729) was consistent with lupeol. Stigmasterol's SMILES required one correction at the final ring junction ([C@H]12C to [C@]12C, a valence error); the corrected string was accepted with site-reported molecular weight 412.702, consistent with stigmasterol. The old pkCSM address (biosig.unimelb.edu.au) returned a certificate error and was not used; all pkCSM predictions come from the current University of Queensland BioSig Lab address.

admetSAR 2.0 (lmmd.ecust.edu.cn/admetsar2) was attempted and failed: the site accepted all submissions, but every result page displayed only a compound list with no endpoint tables, and a benzene control behaved identically, confirming a site display failure rather than a ligand problem. Lupeol was additionally rejected by the site's own reader ("Cannot read this molecule") although the same SMILES works in RDKit and SwissADME. No admetSAR value is reported anywhere in this manuscript, and WP3 therefore rests on ProTox 3.0 and pkCSM, with SwissADME as cross-check.

2.5. WP4 Docking panel and validation

Docking used AutoDock Vina 1.2.5 [4]. Receptor structures were taken from the RCSB Protein Data Bank [12]. Receptors were prepared with Meeko: protein only, with the haem cofactor appended from an OpenBabel-converted cofactor file where present (the hERG, oestrogen-receptor-α and androgen-receptor structures carry no haem). Ligands were prepared with Meeko from the panel SMILES. Each docking used a 24 Å cubic box centred on the co-crystal ligand centroid (or, for hERG, on the pore-site centroid described below), exhaustiveness 32, and five seeds (42, 7, 123, 2024, 555); the best (most negative) score of the five is reported, with the full five-seed values in the deposit pack. Seed-to-seed standard deviations were small (≤ 0.23 kcal/mol across the passing panels), indicating stable sampling.

The panel comprised eight targets: the hERG potassium channel (PDB 7CN1), five cytochrome P450 enzymes relevant to drug metabolism (CYP2C19 4GQS, CYP2C9 1R9O, CYP2D6 4WNT, CYP3A4 2V0M and CYP1A2 2HI4), and the endocrine receptors oestrogen receptor α (ERα, 3ERT) and androgen receptor (AR, 1T65). Validation by re-docking the co-crystal ligand used a root-mean-square deviation (RMSD) criterion of < 2 Å. Table 2 gives the outcome for every target, including the four cases that did not validate cleanly.

Three qualifications govern the panel. First, the hERG structure 7CN1 contains no astemizole coordinates despite its title only potassium ions so re-dock validation on 7CN1 is impossible. The hERG box was therefore centred on the centroid of the Tyr652 and Phe656 side-chain heavy atoms of all four subunits (centre [141.513, 141.431, 167.44]), the pore-site approach, and the missing validation is stated as a limitation wherever hERG results are interpreted. Second, CYP1A2 (2HI4, ligand 7,8-benzoflavone) re-docked at 2.81 Å, failing the < 2 Å criterion; the pose centroid lay only 0.42 Å from the crystal ligand centroid, so the pose occupies the same pocket and the deviation is a near-symmetric orientation flip of a flat ligand. The CYP1A2 panel was run with this limitation stated. Third, the three P450 structures originally specified contain no drug-like ligand at all (CYP2C9 1OG2: haem C and waters only; CYP2D6 2F9Q: haem, sulfate and waters; CYP3A4 1TQN: haem and waters), so validation on them is impossible and the structures were replaced with ligand-bound equivalents verified from the RCSB: CYP2C9 → 1R9O (flurbiprofen), CYP2D6 → 4WNT (AJN), CYP3A4 → 2V0M (ketoconazole). One earlier swap-validation run was discarded after a contaminated receptor file (a duplicated haem block) was detected; the clean re-run reproduced the original validations exactly and is the run reported here.

Interaction extraction used the best-scoring pose (model 1) of each target's strongest binder and the clean receptor file: contacts at ≤ 4.0 Å and hydrogen bonds at ≤ 3.5 Å between oxygen/nitrogen atom pairs, reported per residue with the shortest distance. For the P450 targets these tables report protein contacts only, because the haem cofactor is absent from the clean receptor files; contacts with haem are therefore not captured and this is noted in the corresponding table notes. Pose figures use the tight pocket frame: cartoon only for residues within ~9 Å of the ligand, semi-transparent grey; pocket side chains within ~4.8 Å as slate sticks; the ligand large and central with yellow carbons; hydrogen bonds as yellow dashes.

2.6. Molecular dynamics

Two 10 ns molecular dynamics runs were completed on the strongest soluble complexes that can be built without a haem cofactor: ERα–silybin (completed 2 November 2026) and AR–epicatechin (completed 4 November 2026), each 5,000,000 steps of 2 fs. Simulations used GROMACS 2023.3 with the OPLS-AA force field [18, 19]. Ligand topologies were generated with LigParGen 2.1 [17] using the 1.14*CM1A-LBCC charge model; the docked ligand poses were mapped onto the LigParGen atom order and the mapping was validated by bond lengths. Protein structures were repaired for missing crystal side-chain atoms with PDBFixer and built with neutral NH2/COOH termini. Systems were solvated with SPC water in a dodecahedron box, neutralised and brought to 0.15 M NaCl, energy-minimised, and equilibrated for 100 ps in the NVT ensemble followed by 100 ps in the NPT ensemble, before the 10 ns production run. Trajectories were written every 10 ps (1,001 frames per system) and centred on the protein with periodic-boundary treatment before analysis. Analyses were protein Cα RMSD, ligand RMSD after fitting on protein Cα atoms, per-residue Cα RMSF, protein radius of gyration (Rg) and protein–ligand hydrogen-bond counts and per-residue-pair occupancy. Hydrogen bonds were counted with GROMACS criteria (donor–acceptor distance ≤ 0.35 nm, angle within 30° of linearity); per-residue-pair occupancies were computed on pocket-only trajectories (protein residues within 4.5 Å of the ligand) with the same criteria and are used only to name the dominant anchoring pairs (Section 3.7). The cytochrome P450 complexes could not be run, because the installed OPLS-AA force field contains no

haem parameters and removing haem from the pocket would distort it; this is stated as a limitation in Section 5. LigParGen topologies for kaempferol and lupeol (the CYP-complex ligands) have been generated and are retained for future work.

2.7. WP5 — Safety synthesis

The safety ranking in Section 3.6 is a reasoned synthesis across all predictors and the docking panel, not a composite score and not the output of any single tool. A constituent is flagged for follow-up when independent prediction types converge on the same endpoint (for example, a hERG II prediction together with top hERG docking), when it is the sole carrier of a severe flag (for example, the only GHS Class 3 acute toxicity value), or when predictors disagree in a way that only experiment can resolve. Tiers prioritise experimental work; they do not classify any constituent as safe or toxic.

3. Results

3.1. The panel

Figure 1 shows the twelve panel structures. The panel spans three chemical families: phenolic acids and their esters (chlorogenic, gallic, 4-hydroxybenzoic, caffeic and ferulic acids), flavonoids and related polyphenols (epicatechin, kaempferol, esculin and the reference standard silybin), and lipophilic terpenoids and sterols (lupeol, stigmasterol), with coumarin as a simple benzopyrone. That spread is analytically useful: it lets the safety signals be read against chemistry rather than as isolated flags.

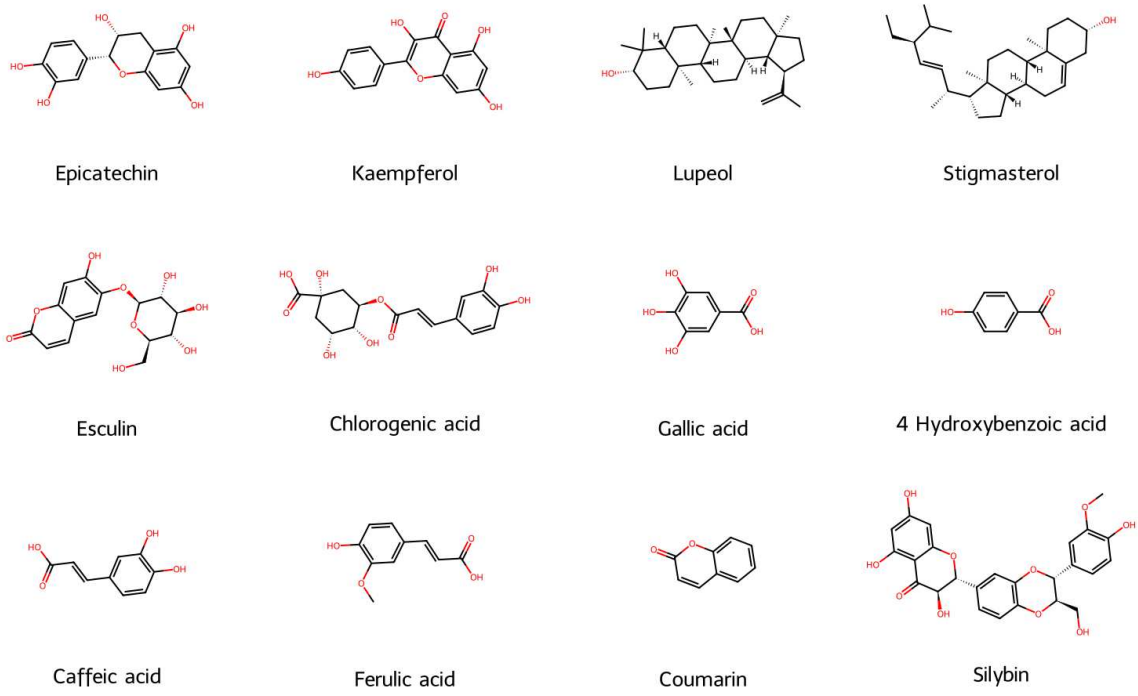


Figure 1. Two-dimensional structures of the twelve panel compounds, drawn from the panel SMILES strings.

3.2. WP1 — Drug-likeness: nine of twelve pass both filters

Compound	MW	logP (Crippen)	TPSA (Å²)	HBD	HBA	RotB	Lipinski violations	Veber
Epicatechin	290.27	1.55	110.38	5	6	1	0	Pass
Kaempferol	286.24	2.28	111.13	4	6	1	0	Pass
Lupeol	426.73	8.02	20.23	1	1	1	1	Pass
Stigmasterol	412.7	7.8	20.23	1	1	5	1	Pass
Esculin	340.28	-1.32	149.82	5	9	3	0	Fail
Chlorogenic acid	354.31	-0.65	164.75	6	8	4	1	Fail
Gallic acid	170.12	0.5	97.99	4	4	1	0	Pass
4-Hydroxybenzoic acid	138.12	1.09	57.53	2	2	1	0	Pass
Caffeic acid	180.16	1.2	77.76	3	3	2	0	Pass
Ferulic acid	194.19	1.5	66.76	2	3	3	0	Pass
Coumarin	146.14	1.79	30.21	0	2	0	0	Pass
Silybin	482.44	2.36	155.14	5	10	4	0	Fail

Table 2. WP1 RDKit descriptors. Lipinski allows one violation; Veber fail = TPSA > 140 Å² or RotB > 10.

Nine compounds pass both the Lipinski and Veber filters [10, 11]. The three exceptions are informative rather than disqualifying. Lupeol (logP 8.02) and stigmasterol (logP 7.80) each carry a single Lipinski violation from excessive lipophilicity, consistent with their triterpenoid/sterol character and with their poor predicted solubility in the SwissADME cross-check (Section 3.4). Chlorogenic acid carries a single Lipinski violation (six hydrogen-bond donors) and fails Veber on polar surface area (164.75 Å²), as do esculin (149.82 Å²) and silybin (155.14 Å²) the three Veber failures, all driven by TPSA above 140 Å². The practical reading is about absorption, not safety: these three are predicted to permeate membranes poorly, which bounds their systemic exposure as free compounds and therefore the weight that should be put on their systemic interaction signals.

3.3. WP2 — Structural alerts: catechols dominate, and they are not toxicity verdicts

Compound	PAINS	Brenk
Epicatechin	catechol_A(92)	catechol
Kaempferol	—	—
Lupeol	—	isolated_alkene
Stigmasterol	—	isolated_alkene
Esculin	—	cumarine
Chlorogenic acid	catechol_A(92)	catechol, Michael_acceptor_1
Gallic acid	catechol_A(92)	catechol

4-Hydroxybenzoic acid	—	—
Caffeic acid	catechol_A(92)	catechol, Michael_acceptor_1
Ferulic acid	—	Michael_acceptor_1
Coumarin	—	cumarine
Silybin	—	—

Table 3. WP2 structural alerts (RDKit FilterCatalog, catalogue-separated).

Four compounds carry the PAINS catechol_A(92) flag epicatechin, chlorogenic acid, gallic acid and caffeic acid and the same four carry the Brenk catechol flag [8, 9]. These are classic polyphenol assay-interference flags: catechols redox-cycle and chelate metals, and they are notorious for false positives in antioxidant and enzyme assays. They are not toxicity verdicts, and they must not be reported as such; their operational consequence is that any future bioassay on these four compounds needs interference controls. Three further Brenk flags appear: Michael_acceptor_1 for chlorogenic acid, caffeic acid and ferulic acid (the α,β-unsaturated carbonyl, a soft-electrophile motif that warrants a reactivity note but is common in dietary phenolics), isolated_alkene for lupeol and stigmasterol, and cumarine for esculin and coumarin. Three compounds are completely clean under both catalogues: kaempferol, 4-hydroxybenzoic acid and silybin.

3.4. WP3 — Toxicity prediction: two predictors, two disagreements, one failure

SwissADME cross-check

SwissADME agreed with RDKit exactly on Veber, failing the same three compounds (esculin, chlorogenic acid and silybin, all TPSA > 140 Å²), and passed all twelve on Lipinski, with single violations noted for lupeol and stigmasterol (MLOGP > 4.15) and chlorogenic acid (NHorOH > 5) consistent with the RDKit result, since Lipinski allows one violation. Predicted GI absorption was high for seven compounds (epicatechin, kaempferol, gallic acid, 4-hydroxybenzoic acid, caffeic acid, ferulic acid and coumarin) and low for four (stigmasterol, esculin, chlorogenic acid and silybin). Only three compounds were predicted BBB-permeant: 4-hydroxybenzoic acid, ferulic acid and coumarin. Lupeol and stigmasterol were predicted poorly soluble. One SwissADME result is unconfirmed and is reported as such: in the batch run, lupeol's GI absorption, BBB permeation and iLOGP values exactly duplicated the preceding compound (kaempferol), and a single-compound rerun left those three fields blank. They are therefore reported as NOT CONFIRMED in the deposit pack and are not used anywhere in this manuscript; no substitute value has been filled in from any other tool.

ProTox 3.0

Compound	LD50 (mg/kg)	GHS class	Hepato-	Neuro-	Nephro-	Cardio-	Carcino-	Immuno-	Mutagenicity (Ames)
Epicatechin	10000	6	Inactive	Inactive	Active (0.62)	Inactive	Inactive	Inactive	Inactive
Kaempferol	3919	5	Inactive	Inactive	Active (0.62)	Inactive	Inactive	Inactive	Inactive
Lupeol	2000	4	Inactive	Active (0.54)	Inactive	Inactive	Inactive	Active (0.57)	Inactive

Stigmasterol	890	4	Inactive	Active (0.54)	Inactive	Inactive	Inactive	Active (0.99)	Inactive
Esculin	4000	5	Inactive	Inactive	Active (0.73)	Inactive	Inactive	Active (0.70)	Inactive
Chlorogenic acid	5000	5	Inactive	Inactive	Active (0.56)	Inactive	Inactive	Active (0.99)	Inactive
Gallic acid	2000	4	Inactive	Inactive	Active (0.69)	Inactive	Active (0.56)	Inactive	Inactive
4-Hydroxybenzoic acid	2200	5	Inactive	Inactive	Active (0.68)	Inactive	Inactive	Inactive	Inactive
Caffeic acid	2980	5	Inactive	Inactive	Active (0.59)	Inactive	Active (0.78)	Inactive	Inactive
Ferulic acid	1772	4	Inactive	Inactive	Active (0.62)	Inactive	Inactive	Active (0.91)	Inactive
Coumarin	196	3	Inactive	Active (0.58)	Inactive	Inactive	Active (0.83)	Inactive	Inactive
Silybin	2000	4	Inactive	Inactive	Active (0.68)	Active (0.72)	Inactive	Active (0.97)	Inactive

Table 4. ProTox 3.0 predictions (accessed 25 October 2026; structures resolved via the site's PubChem-name search, not SMILES-typed see Section 2.4). Probabilities shown for Active flags; all other probabilities are in the deposit pack. GHS classes as shown on the site (III: 50–300; IV: 300–2000; V: 2000–5000; VI: > 5000 mg/kg).

Two ProTox results are unanimous and reassuring as far as predictions go: hepatotoxicity was predicted inactive for all twelve compounds, and mutagenicity (Ames) was predicted inactive for all twelve. The acute-toxicity spread is wide. Coumarin has the lowest predicted LD50 by a large margin (196 mg/kg, the only GHS Class 3 value in the panel) and epicatechin the highest (10000 mg/kg, Class 6); the remaining compounds fall in Classes 4–5. Cardiotoxicity was predicted active for exactly one compound, silybin (0.72). Carcinogenicity was predicted active for three: gallic acid (0.56), caffeic acid (0.78) and coumarin (0.83). Nephrotoxicity was predicted active for nine of twelve, inactive only for lupeol, stigmasterol and coumarin. Neurotoxicity was predicted active for the same three lipophilic compounds at borderline probabilities (lupeol 0.54, stigmasterol 0.54, coumarin 0.58) flags to note, not findings, given their distance from confident prediction. Immunotoxicity was predicted active for six compounds (lupeol, stigmasterol, esculin, chlorogenic acid, ferulic acid and silybin). Among the Tox21 nuclear-receptor and MIE flags, three patterns stand out: kaempferol (aryl hydrocarbon receptor 1.0, aromatase 0.96, oestrogen receptor 1.0, ER ligand-binding domain 0.95), caffeic acid (androgen receptor 1.0) and silybin (aryl hydrocarbon receptor 0.99, transthyretin 0.92), with esculin also flagging transthyretin (0.92) and acetylcholinesterase (0.65). One data-quality pattern is recorded honestly: many MIE probabilities repeat identically across ligands (for example, THRα 0.90, THRβ 0.78, RYR 0.98, KAR 0.99), which suggests shared model baselines rather than compound-specific signal, and those repeated values are not interpreted further here.

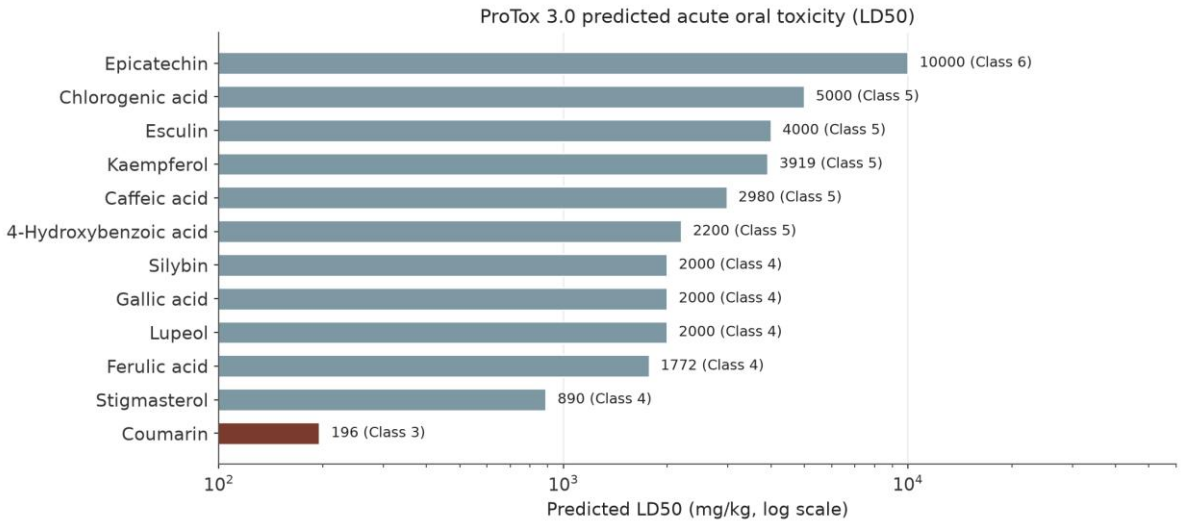


Figure 2. ProTox 3.0 predicted acute oral LD50 values (log scale) with GHS classes. Coumarin is the only Class 3 compound; epicatechin the least acutely toxic by this predictor.

pkCSM

Compound	AMES	hERG I	hERG II	Hepatotoxicity	Skin sensitisation	LD50 (mol/kg)	LOAEL (log mg/kg/day)	Max. tolerated dose (log mg/kg/day)
Epicatechin	Yes	No	No	No	No	2.101	2.076	0.956
Kaempferol	Yes	No	No	No	No	2.312	1.981	1.069
Lupeol*	No	No	Yes	No	No	2.065	1.021	0.454
Stigmasterol*	No	No	Yes	No	No	2.032	0.938	0.597
Esculin	Yes	No	No	Yes	No	1.775	1.635	0.628
Chlorogenic acid	No	No	No	No	No	1.514	1.799	0.572
Gallic acid	No	No	No	No	No	1.872	1.499	1.404
4-Hydroxybenzoic acid	No	No	No	No	No	2.022	2.875	1.541
Caffeic acid	No	No	No	No	No	1.910	3.070	1.431
Ferulic acid	No	No	No	No	No	1.954	2.892	1.366
Coumarin	No	No	No	No	No	2.286	1.912	1.484
Silybin	No	No	Yes	No	No	2.184	2.593	0.307

*Table 5. pkCSM predictions (current BioSig Lab address, accessed 25 October 2026; single-molecule mode). * Lupeol run on connectivity-only SMILES; stigmasterol SMILES corrected at the ring junction (see Section 2.4). pkCSM LD50 units (mol/kg) differ from ProTox units (mg/kg) and the two must not be compared directly.*

pkCSM was unanimous on two endpoints: skin sensitisation was predicted negative for all twelve compounds, and hERG I inhibition was predicted negative for all twelve. Its hERG II predictions, however, singled out exactly three compounds lupeol, stigmasterol and silybin and those are the same

three that topped the hERG docking panel (Section 3.5). That is a qualitative agreement between two independent prediction types, and it is reported as such: it is not proof of hERG blockade, which only electrophysiology could establish. Hepatotoxicity was predicted positive for exactly one compound, esculin. On the continuous endpoints, the lowest predicted LD50 was chlorogenic acid (1.514 mol/kg) and the highest kaempferol (2.312 mol/kg); the lowest LOAEL values were stigmasterol (0.938) and lupeol (1.021 log mg/kg/day); and the lowest maximum tolerated doses were silybin (0.307) and lupeol (0.454 log mg/kg/day).

Where the predictors disagree both sides reported

Two disagreements matter and neither is resolved here. First, AMES: pkCSM predicts mutagenicity for epicatechin, kaempferol and esculin, while ProTox 3.0 predicts mutagenicity inactive for all twelve (epicatechin 0.55, kaempferol 0.52, esculin 0.73). Second, hepatotoxicity: pkCSM predicts it positive for esculin alone, while ProTox 3.0 predicts it inactive for all twelve (esculin 0.86). A reader who saw only one predictor would reach opposite conclusions for these compounds; the honest statement is that the Ames status of three compounds and the hepatotoxicity status of one are unresolved by prediction and require an experimental Ames test and a hepatotoxicity assay respectively. The admetSAR 2.0 failure (Section 2.4) means no third predictor is available to break either tie in this version.

3.5. WP4 — Docking: a selective, target-specific pattern

Target	PDB used	Co-crystal ligand	Re-dock RMSD (Å)	Outcome
hERG	7CN1	— (no ligand coordinates)	Impossible (no ligand in file)	Pore-site box (see text)
CYP2C19	4GQS	0XV	0.68	Pass
CYP2C9	1R9O (swap for apo 1OG2)	FLP (flurbiprofen)	1.20	Pass
CYP2D6	4WNT (swap for apo 2F9Q)	AJN	1.41	Pass
CYP3A4	2V0M (swap for apo 1TQN)	KLN (ketoconazole)	1.26	Pass
CYP1A2	2HI4	BHF (7,8-benzoflavone)	2.81	Fail same pocket, symmetric flip (centroid 0.42 Å); panel run with limitation
ERα	3ERT	OHT (4-hydroxytamoxifen)	1.59	Pass
AR	1T65	DHT	0.41	Pass (chosen over 2AM9/TES, 0.47 Å)

Table 6. WP4 validation outcomes (AutoDock Vina 1.2.5, 24 Å box, exhaustiveness 32, seed 42; criterion RMSD < 2 Å).

Six of the eight targets validated cleanly, including the androgen receptor at 0.41 Å the best in the panel and CYP2C19 at 0.68 Å. The two exceptions are stated in the table and carried as limitations throughout: hERG could not be validated at all, and CYP1A2 validated only as a same-pocket flip. The three structure swaps were validated cleanly on re-run (1.20, 1.41 and 1.26 Å).

Compound	hERG	CYP2C19	CYP2C9	CYP2D6	CYP3A4	CYP1A2	ERα	AR
Epicatechin	-7.69	-8.40	-8.11	-7.68	-8.13	-9.78	-8.23	-8.60
Kaempferol	-7.82	-7.93	-8.05	-8.65	-8.08	-10.60	-8.10	-8.35
Lupeol	-9.09	-9.78	-6.72	NB (+1.68)	-10.50	NB (+1.82)	-8.68	NB (+2.75)
Stigmasterol	-7.94	-9.96	-9.69	-6.90	-10.08	-4.47	-8.16	-1.02*
Esculin	-7.80	-8.46	-8.32	-8.60	-8.19	-8.58	-8.48	-7.61
Chlorogenic acid	-7.98	-8.34	-8.32	-8.97	-8.27	-7.85	-7.36	-7.81
Gallic acid	-5.44	-5.49	-5.78	-6.43	-5.34	-6.84	-5.55	-5.83
4-Hydroxybenzoic acid	-4.80	-5.50	-5.46	-6.19	-5.49	-6.76	-5.52	-5.76
Caffeic acid	-5.79	-6.34	-6.01	-6.98	-6.37	-7.66	-6.36	-6.68
Ferulic acid	-6.02	-6.14	-6.22	-6.96	-6.63	-7.79	-6.25	-6.45
Coumarin	-5.54	-6.79	-6.54	-7.70	-6.73	-8.48	-6.22	-7.20
Silybin	-8.93	-9.51	-9.42	-7.50	-9.85	NB (+10.15)	-9.29	NB (+9.28)

*Table 7. Best docking scores (kcal/mol; best of five seeds) for every ligand–target pair. NB = non-binder (positive score). * Stigmasterol–AR (−1.02) is effectively non-binding. Full five-seed values, means and standard deviations are in the deposit pack.*

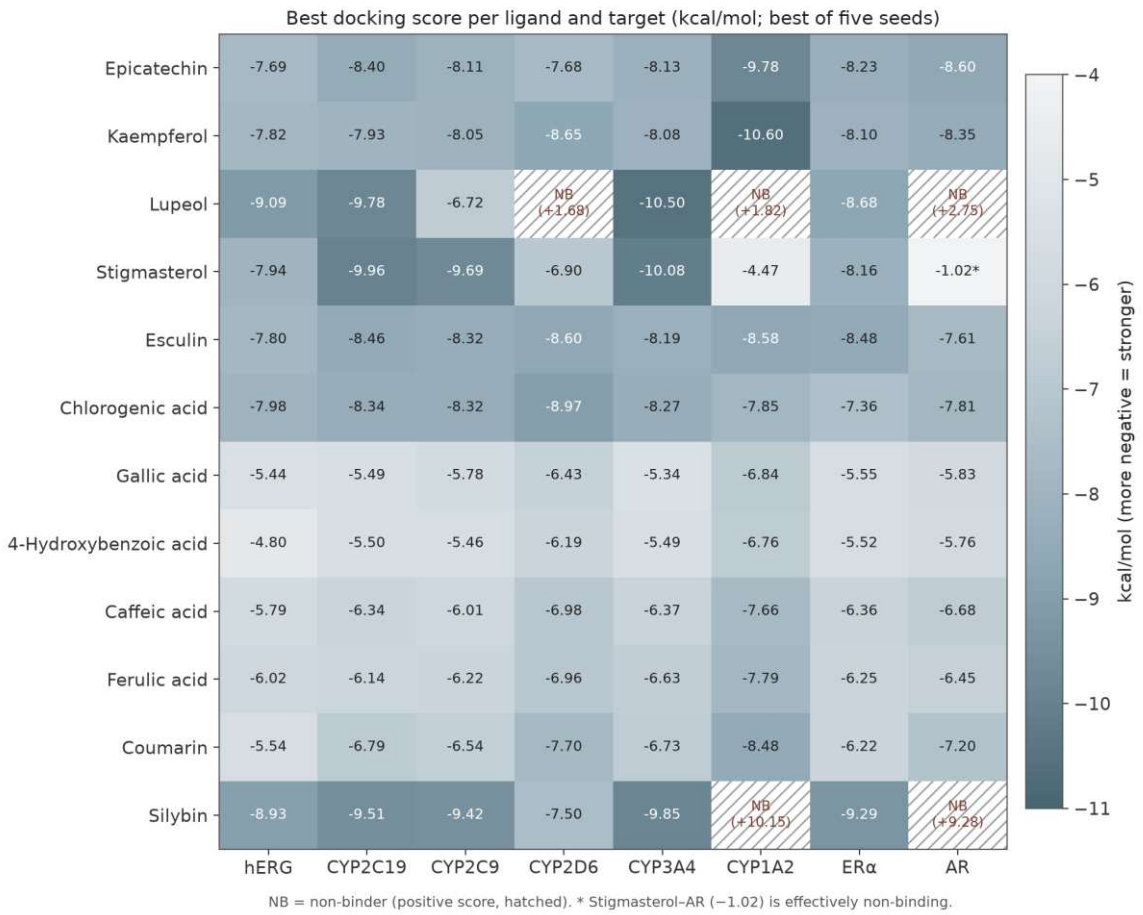


Figure 3. Heatmap of best docking scores (kcal/mol). Darker cells are stronger predicted binding; hatched cells are non-binders. The pattern is target-specific, not a uniform lipophilicity effect (see text).

hERG: the cardiac signal

Lupeol is the strongest predicted hERG binder in the panel (−9.09 kcal/mol), followed by silybin (−8.93), chlorogenic acid (−7.98), stigmasterol (−7.94), kaempferol (−7.82), esculin (−7.80) and epicatechin (−7.69); the weakest are gallic acid (−5.44) and 4-hydroxybenzoic acid (−4.80). The lupeol pose sits on the pore axis, contacting Tyr652 of all four subunits and Ser624 of three, with hydrogen bonds to Tyr652 (chain C, 3.19 Å) and Ser624 (chain C, 3.31 Å) the pore-lining residues around which the box was centred. Because the hERG model could not be validated (Section 2.5), these scores carry wider uncertainty than the validated targets, and the convergence with the pkCSM hERG II predictions for lupeol, stigmasterol and silybin is the strongest reason to prioritise those three for electrophysiology rather than any single score.

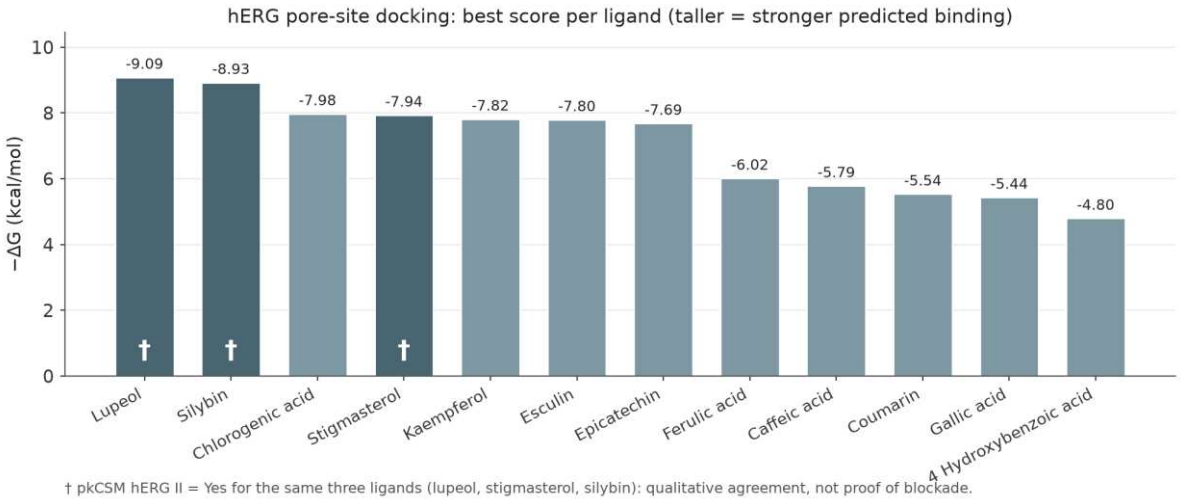


Figure 4. hERG pore-site docking, plotted as −ΔG so that taller bars mean stronger predicted binding. Daggers mark the three pkCSM hERG II positives.

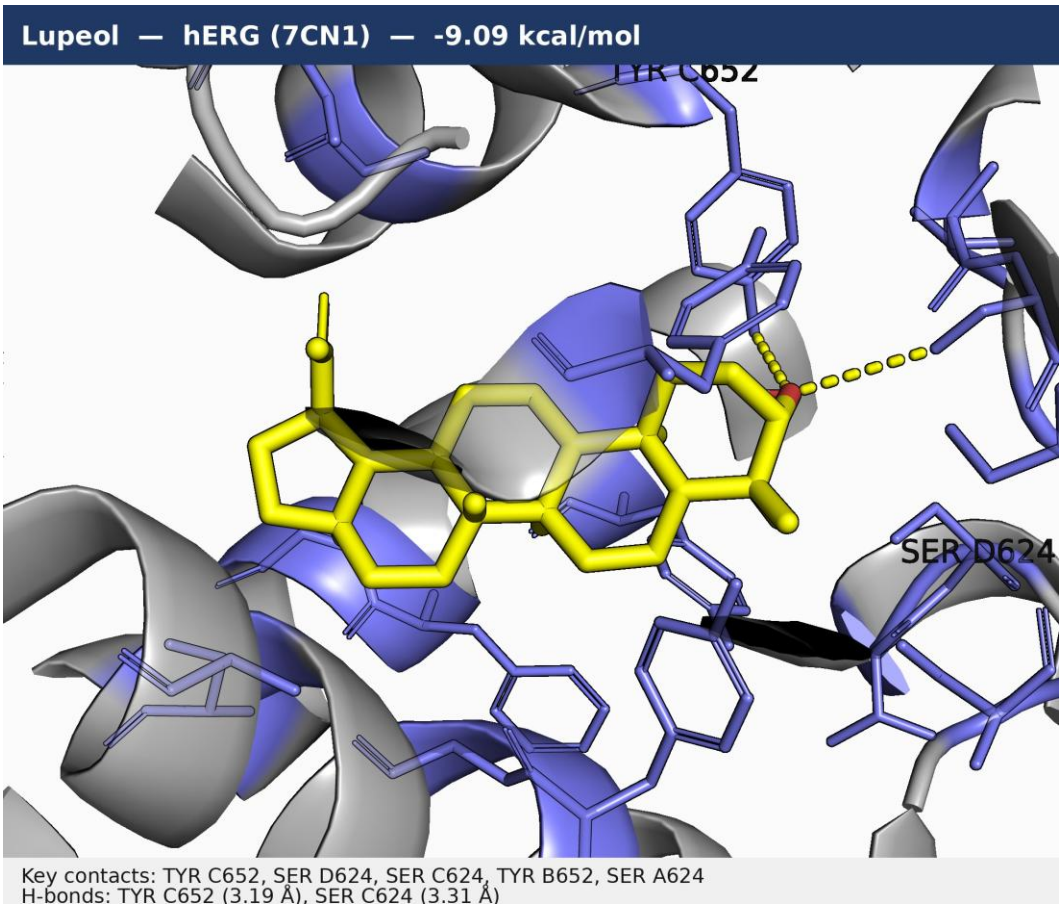


Figure 5. Tight-frame pose of lupeol in the hERG pore (7CN1), −9.09 kcal/mol. Grey semi-transparent cartoon: residues within ~9 Å; slate sticks: pocket side chains; yellow carbons: ligand; yellow dashes: hydrogen bonds.

Cytochrome P450 enzymes: strong binding, and strong selectivity

CYP3A4 produced the strongest single score in the whole panel for a P450 target after CYP1A2: lupeol at −10.50 kcal/mol, followed by stigmasterol (−10.08) and silybin (−9.85); the weakest CYP3A4 binder was gallic acid (−5.34). CYP2C19 was led by stigmasterol (−9.96), lupeol (−9.78) and silybin (−9.51), with gallic acid and 4-hydroxybenzoic acid weakest (−5.49 and −5.50). CYP2C9 was led by stigmasterol (−9.69) and silybin (−9.42), with 4-hydroxybenzoic acid weakest (−5.46). CYP2D6 was led by chlorogenic acid (−8.97), kaempferol (−8.65) and esculin (−8.60), and is the panel in which lupeol is a non-binder (+1.68). CYP1A2 produced the strongest score in the entire study, kaempferol at −10.60 kcal/mol, followed by epicatechin (−9.78), esculin (−8.58) and coumarin (−8.48); it is also the panel with the two clearest non-binders, silybin (+10.15) and lupeol (+1.82), and the weakest binder, stigmasterol (−4.47). The CYP1A2 scores must be read with the flip limitation in mind, but the rank order within the panel is unaffected by a symmetric flip of the validation ligand, which concerns the reference pose rather than the panel compounds.

The selectivity pattern is the most informative feature of the panel. Lupeol is a non-binder at AR, CYP2D6 and CYP1A2 yet the strongest binder at CYP3A4 and hERG. Silybin is a non-binder at AR and CYP1A2 yet the strongest binder at ERα and among the strongest at CYP3A4 and CYP2C9. A generic hydrophobic-stickiness artefact would not produce this pattern; it would bind everywhere. What the pattern suggests as a hypothesis for experimental testing, not a conclusion is pocket-specific complementarity, which is precisely why the strong CYP3A4 and CYP1A2 scores deserve inhibition assays while the non-binding results deserve to be reported with equal prominence.

Endocrine receptors: one strong binder each, and two non-binders that matter

At ERα, silybin is the strongest binder (−9.29 kcal/mol), followed by lupeol (−8.68), esculin (−8.48), epicatechin (−8.23), stigmasterol (−8.16) and kaempferol (−8.10); the weakest are gallic acid (−5.55) and 4-hydroxybenzoic acid (−5.52). The silybin pose is anchored by three hydrogen bonds (Glu353, 2.70 Å; Arg394, 2.96 Å; Thr347, 2.97 Å) among nineteen contacts. At AR, epicatechin is the strongest binder (−8.60 kcal/mol), followed by kaempferol (−8.35) and chlorogenic acid (−7.81), with four hydrogen bonds (Leu873, 2.90 Å; Gln711, 2.91 Å; Thr877, 3.12 Å; Met745, 3.28 Å). The AR panel's most important results are its negatives: silybin (+9.28) and lupeol (+2.75) are non-binders, and stigmasterol (−1.02) is effectively non-binding. Binding is not agonism or antagonism, and no functional claim is made here; the finding is that these compounds are predicted to occupy the hormone-binding pockets, which is the necessary first condition for endocrine activity and the reason reporter-gene assays are proposed for kaempferol, silybin and epicatechin in Section 6.

Top-complex interactions

Target	Strongest binder	Score (kcal/mol)	Contacts (≤ 4.0 Å)	Hydrogen bonds (≤ 3.5 Å)
CYP2C19 (4GQS)	Stigmasterol	-9.96	18	none ≤ 3.5 Å
CYP2C9 (1R9O)	Stigmasterol	-9.69	16	THR A304 (3.09 Å); GLU A300 (3.48 Å)
CYP2D6 (4WNT)	Chlorogenic acid	-8.97	19	GLU A216 (2.91 Å); GLN A244 (3.02 Å); ALA A305 (3.12 Å);

				ASP A301 (3.14 Å); SER A304 (3.19 Å); ALA A300 (3.25 Å); LEU A213 (3.38 Å)
CYP3A4 (2V0M)	Lupeol	-10.50	10	none ≤ 3.5 Å
CYP1A2 (2HI4)	Kaempferol	-10.60	18	ASP A313 (3.23 Å)
ERa (3ERT)	Silybin	-9.29	19	GLU A353 (2.7 Å); ARG A394 (2.96 Å); THR A347 (2.97 Å)
AR (1T65)	Epicatechin	-8.60	15	LEU A873 (2.9 Å); GLN A711 (2.91 Å); THR A877 (3.12 Å); MET A745 (3.28 Å)

Table 8. Top complex per target with interaction counts. Full per-residue contact lists with minimum distances are in the deposit pack. CYP rows report protein contacts only (haem absent from the clean receptor files). hERG–lupeol: 11 contacts, hydrogen bonds to Tyr652 (chain C, 3.19 Å) and Ser624 (chain C, 3.31 Å).

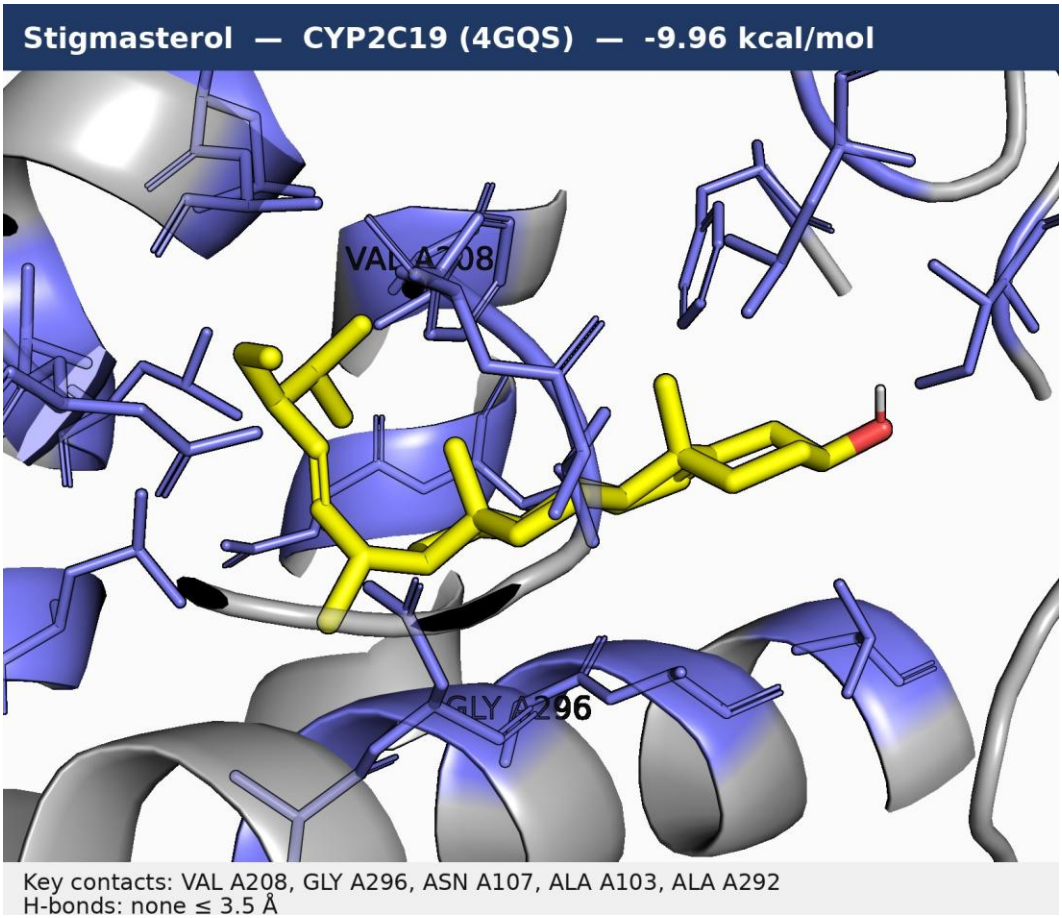


Figure 6. Tight-frame pose of stigmasterol in CYP2C19 (4GQS), −9.96 kcal/mol. No hydrogen bond ≤ 3.5 Å; protein contacts only (haem absent from the clean receptor file).

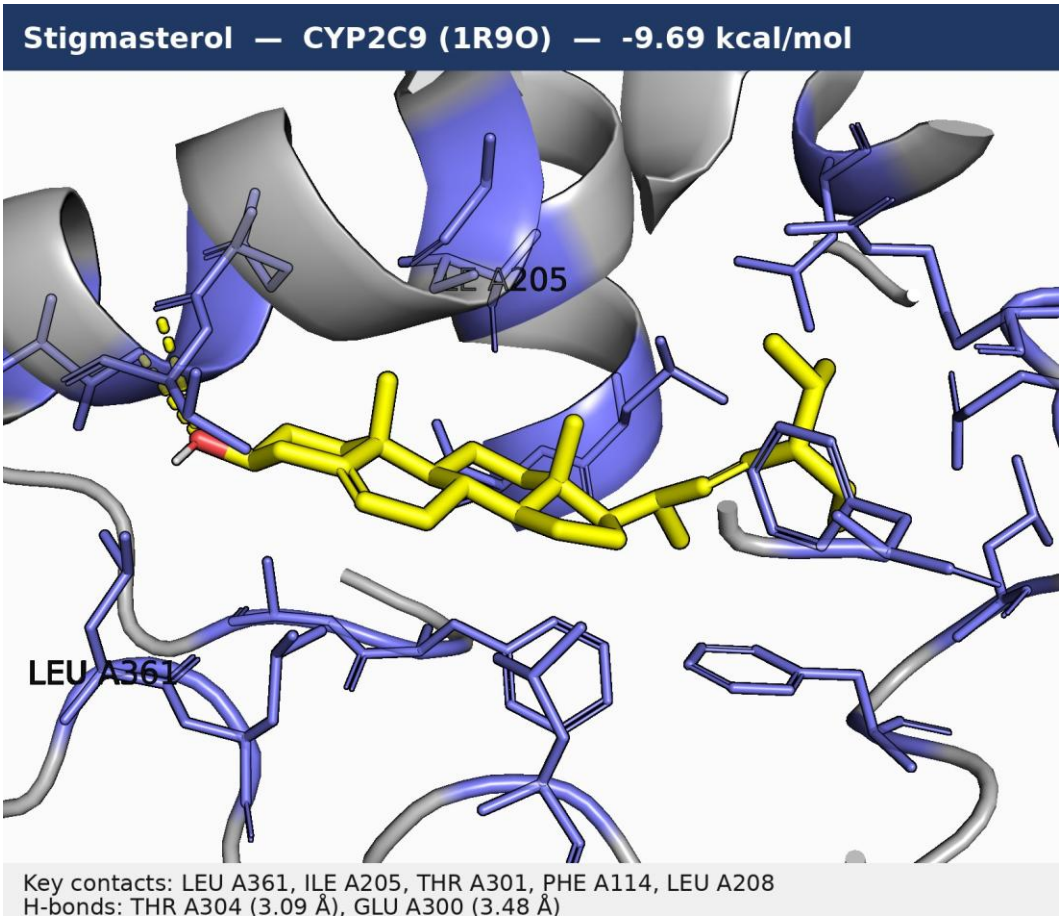


Figure 7. Tight-frame pose of stigmasterol in CYP2C9 (1R9O), −9.69 kcal/mol. Hydrogen bonds to Thr304 (3.09 Å) and Glu300 (3.48 Å); protein contacts only (haem absent from the clean receptor file).

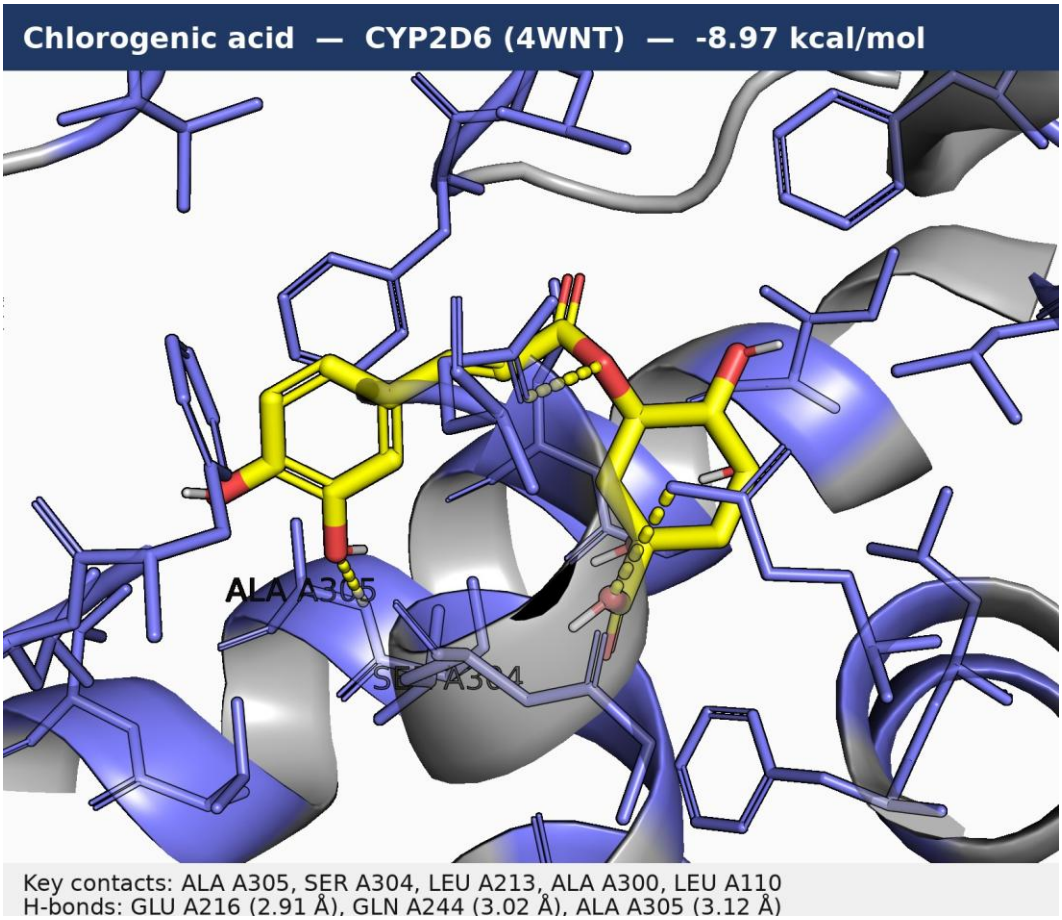


Figure 8. Tight-frame pose of chlorogenic acid in CYP2D6 (4WNT), −8.97 kcal/mol. Seven hydrogen bonds, shortest to Glu216 (2.91 Å); protein contacts only (haem absent from the clean receptor file).

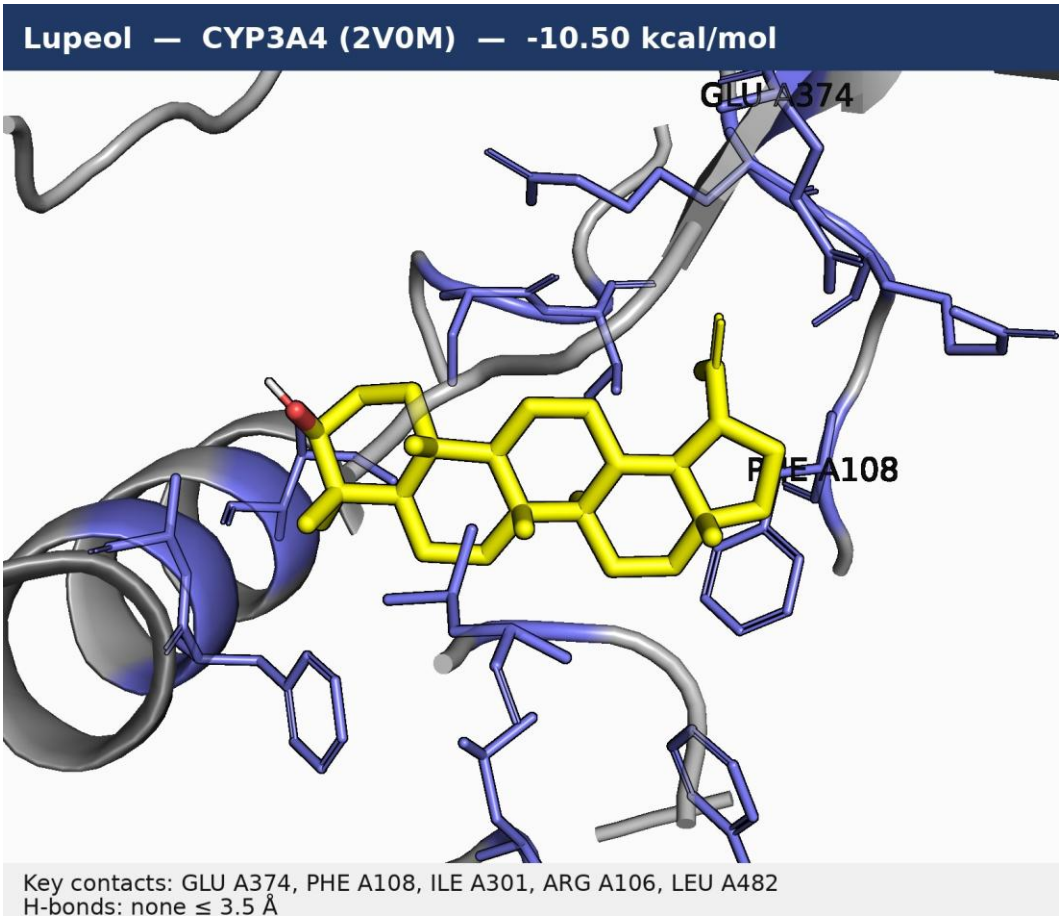


Figure 9. Tight-frame pose of lupeol in CYP3A4 (2V0M), −10.50 kcal/mol. No hydrogen bond ≤ 3.5 Å; protein contacts only (haem absent from the clean receptor file).

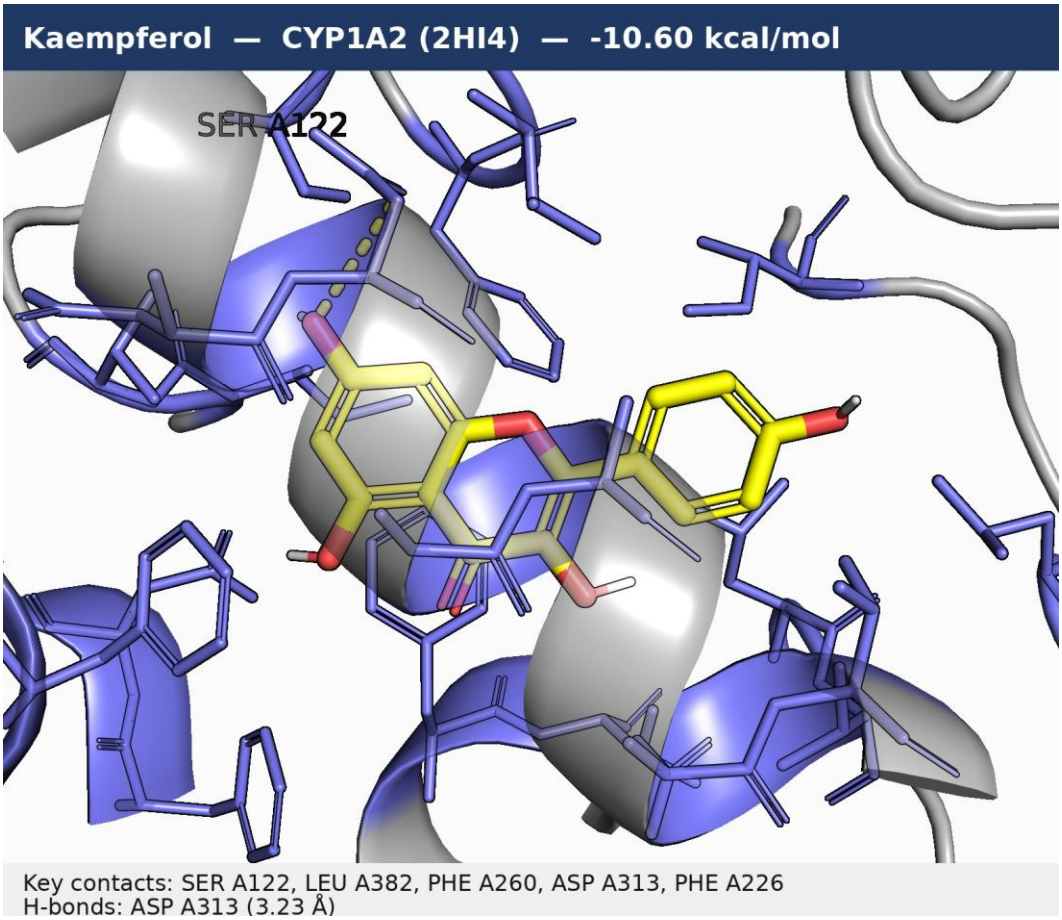


Figure 10. Tight-frame pose of kaempferol in CYP1A2 (2HI4), −10.60 kcal/mol, the strongest score in the study. One hydrogen bond, to Asp313 (3.23 Å); protein contacts only (haem absent from the clean receptor file). Read with the CYP1A2 flip limitation.

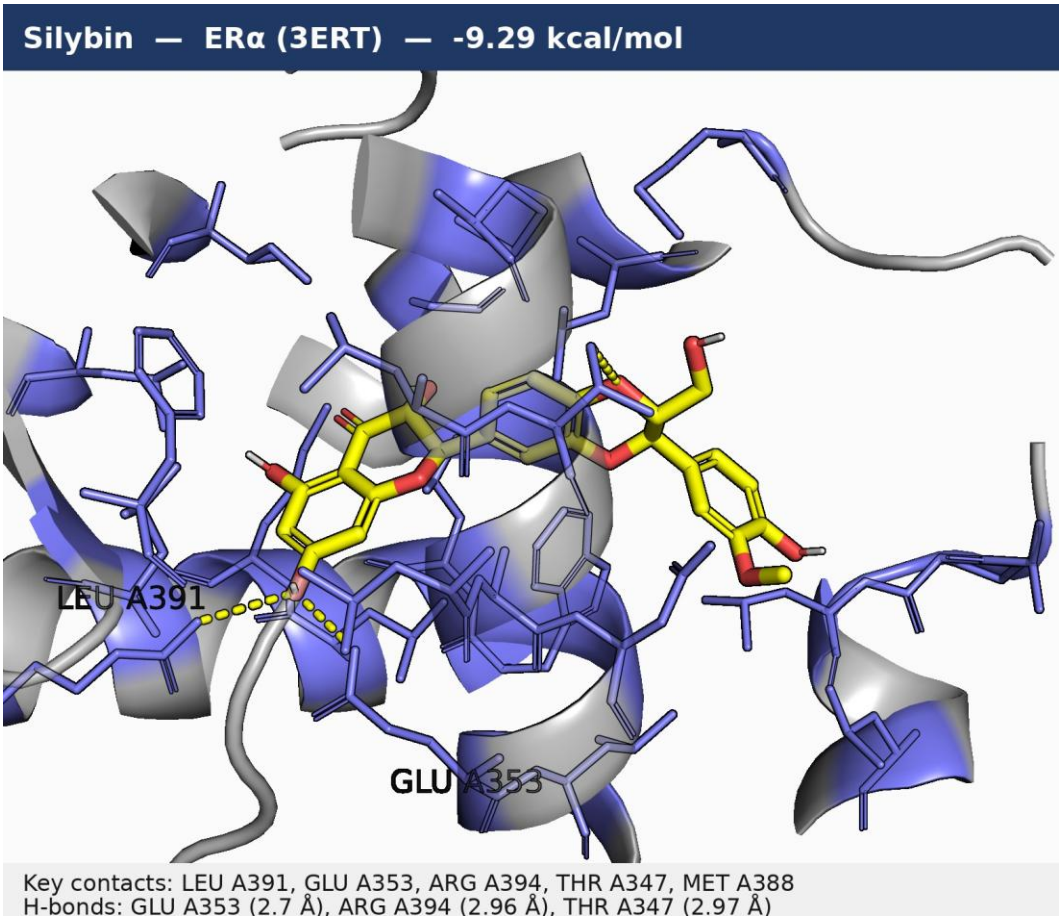


Figure 11. Tight-frame pose of silybin in ERα (3ERT), −9.29 kcal/mol. Hydrogen bonds to Glu353 (2.70 Å), Arg394 (2.96 Å) and Thr347 (2.97 Å).

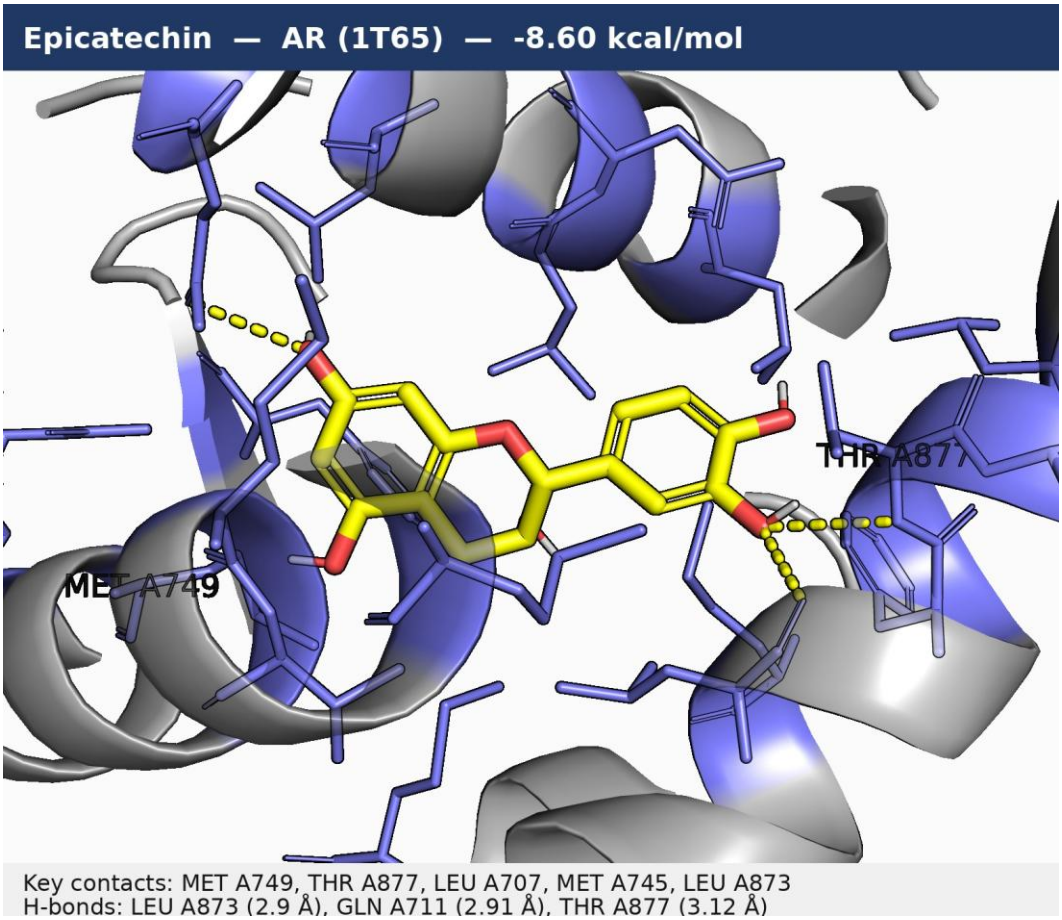


Figure 12. Tight-frame pose of epicatechin in AR (1T65), −8.60 kcal/mol. Hydrogen bonds to Leu873 (2.90 Å), Gln711 (2.91 Å), Thr877 (3.12 Å) and Met745 (3.28 Å).

3.6. WP5 — Safety synthesis: a prioritised ranking, not a verdict

No single score ranks these compounds, and any ranking that pretended otherwise would hide the disagreements that are the most decision-relevant findings. The tiers below prioritise experimental work. They do not classify any compound as safe or toxic, and every tier assignment is conditional on the limitations in Section 5.

Tier	Compounds	Basis (predictions only)	Proposed follow-up
Follow up first	Lupeol; stigmasterol; silybin	hERG II positive (pkCSM) AND top hERG docking; silybin also carries the only cardiotoxicity flag (0.72). Lupeol and stigmasterol also carry borderline neurotoxicity flags (0.54).	hERG patch-clamp; cardiac follow-up before any systemic use.
Follow up first	Coumarin	Lowest predicted LD50 (196 mg/kg, only GHS Class 3); carcinogenicity flag (0.83); borderline neurotoxicity (0.58). Counterweight: weak hERG binding (−5.54), hERG	Acute oral toxicity study; Ames and carcinogenicity follow-up.

		I/II negative, skin sensitisation negative.	
Resolve by experiment	Esculin	Predictors disagree on hepatotoxicity (pkCSM Yes vs ProTox inactive) and on AMES (pkCSM Yes vs ProTox inactive). Veber fail (poor permeability) bounds systemic exposure.	Ames test; hepatotoxicity assay.
Resolve by experiment	Kaempferol	AMES disagreement (pkCSM Yes vs ProTox inactive); endocrine MIE flags (AhR 1.0, ER 1.0, aromatase 0.96, ER-LBD 0.95); strongest CYP1A2 binder (−10.60). Counterweight: clean PAINS/Brenk; no ProTox organ-toxicity flags.	Ames test; CYP1A2 inhibition assay; endocrine reporter assays.
Resolve by experiment	Epicatechin	AMES disagreement (pkCSM Yes vs ProTox inactive). Counterweight: highest predicted LD50 (10000 mg/kg, Class 6); no cardiotoxicity, hepatotoxicity or carcinogenicity flags; strongest AR binder (−8.60).	Ames test.
Lower predicted concern, with noted cautions	Gallic acid; 4-hydroxybenzoic acid; caffeic acid; ferulic acid; chlorogenic acid	Gallic acid: carcinogenicity flag (0.56) but weak binding and no hERG signal. 4-Hydroxybenzoic acid: weakest hERG binder (−4.80) but predicted BBB-permeant. Caffeic acid: carcinogenicity flag (0.78), AR MIE flag (1.0) and Michael-acceptor alert. Ferulic acid: Michael-acceptor alert; nephrotoxicity and immunotoxicity flags. Chlorogenic acid: Veber fail; Michael-acceptor alert; strongest CYP2D6 binder (−8.97).	Routine screening; CYP2D6 inhibition assay for chlorogenic acid; interference controls for the catechols.

Table 9. WP5 prioritised safety ranking. Tiers order experimental work; they are not safety classifications.

Three cross-cutting observations emerge from the ranking. First, the hERG convergence is the strongest multi-tool signal in the study: two independent prediction types agree on the same three compounds, and those three are also the most lipophilic large compounds in the panel, which is the expected chemistry for pore binding but the hERG model is unvalidated, so this remains a prioritisation signal, not a finding. Second, the predictor disagreements are concentrated exactly where they are most consequential (mutagenicity and hepatotoxicity), which is why the Ames test and hepatotoxicity assays

head the experimental list rather than any further computation. Third, the selectivity pattern of Section 3.5 cuts both ways for risk: it argues against dismissing strong scores as generic stickiness, but it also means no compound can be cleared on the basis of a non-binding result at one target when it binds strongly at another.

3.7. Molecular dynamics: both complexes remain bound over 10 ns

Both 10 ns production runs completed without the ligand leaving the pocket. The androgen receptor complex was the steadier of the two: its protein Cα RMSD averaged 0.131 nm (maximum 0.168 nm) with no drift between halves (0.134 nm first half, 0.128 nm second half), and its radius of gyration stayed within 1.844–1.891 nm (mean 1.867 nm). The ERα complex was stable but less quiet: its Cα RMSD averaged 0.232 nm (maximum 0.317 nm), rising from 0.211 nm in the first half to 0.253 nm in the second after a step at ~7.5 ns to a plateau near 0.29 nm, while its radius of gyration compacted slightly (1.909 nm first half to 1.895 nm second half; mean 1.902 nm, range 1.866–1.943 nm) a modest conformational adjustment, not unfolding. Per-residue fluctuation was low in both systems (mean Cα RMSF 0.118 nm for ERα and 0.073 nm for AR); the only large fluctuations were the termini and the ERα C-terminal tail (residues 242–247, up to 0.808 nm), which carry no ligand contacts. The ligands themselves stayed in place: ligand RMSD after fitting on protein Cα atoms averaged 0.176 nm (maximum 0.333 nm) for silybin and 0.157 nm (maximum 0.252 nm) for epicatechin, and the minimum ligand–protein heavy-atom distance never exceeded 0.234 nm (ERα) or 0.278 nm (AR) in any frame, so contact was continuous throughout both runs.

Quantity	ERα–silybin	AR–epicatechin
Protein Cα RMSD, mean (max), nm	0.232 (0.317)	0.131 (0.168)
Protein Cα RMSD, second-half mean, nm	0.253	0.128
Protein Rg, mean (range), nm	1.902 (1.866–1.943)	1.867 (1.844–1.891)
Cα RMSF, mean (peak), nm	0.118 (0.808, C-terminal tail)	0.073 (0.331, termini)
Ligand RMSD after protein fit, mean (max), nm	0.176 (0.333)	0.157 (0.252)
Protein–ligand H-bonds, mean per frame (distinct)	1.70 (13)	2.26 (12)
Frames with ≥ 1 protein–ligand H-bond	100.0%	97.5%
Minimum ligand–protein contact, largest value, nm	0.234	0.278

Table 10. Molecular dynamics summary (10 ns production, 1,001 frames each; GROMACS 2023.3, OPLS-AA). Ligand RMSD is computed after fitting on protein Cα atoms, against the first production frame; hydrogen bonds use GROMACS criteria (donor–acceptor ≤ 0.35 nm, angle within 30° of linearity).

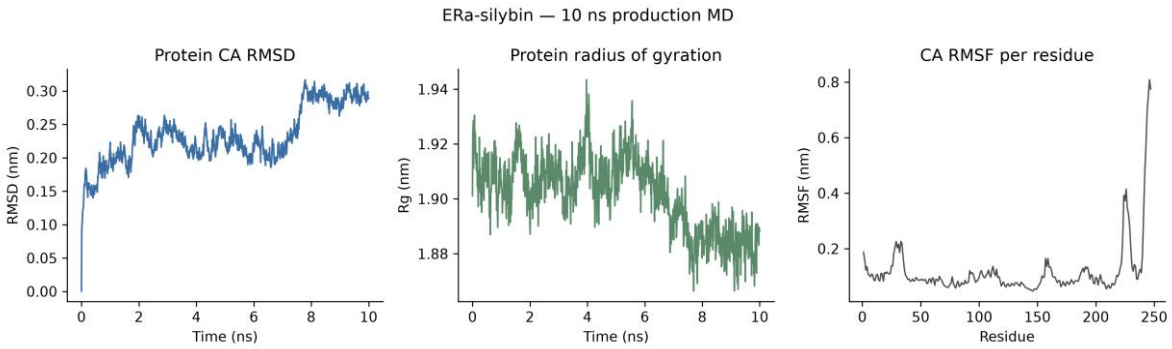


Figure 13. ERα–silybin, 10 ns production molecular dynamics: protein Cα RMSD, protein radius of gyration and per-residue Cα RMSF. The RMSD step at ~7.5 ns and the C-terminal RMSF peak (residues 242–247) are discussed in Section 3.7.

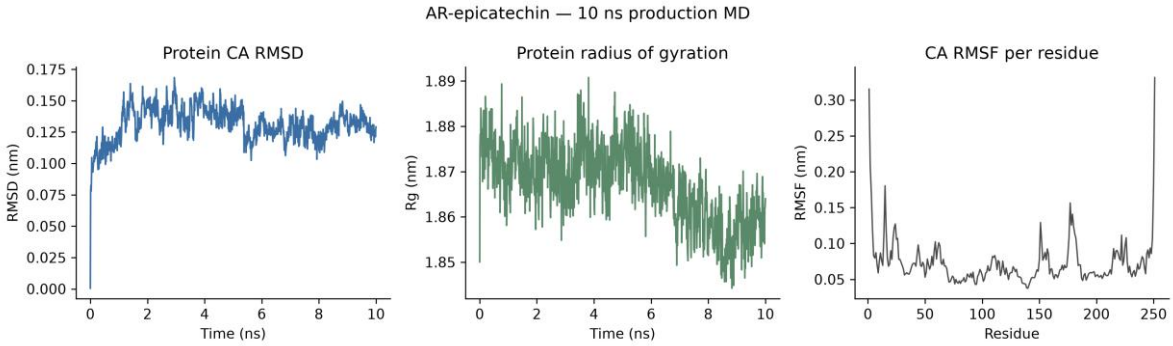


Figure 14. AR–epicatechin, 10 ns production molecular dynamics: protein Cα RMSD, protein radius of gyration and per-residue Cα RMSF. Fluctuation is confined to the termini.

Hydrogen bonding was present in essentially every frame of both runs (GROMACS means 1.70 hydrogen bonds per frame for ERα–silybin and 2.26 for AR–epicatechin; at least one protein–ligand hydrogen bond in 100.0% and 97.5% of frames, respectively). The anchoring pairs, identified from pocket-restricted per-residue-pair occupancies, are listed in Table 11. The ERα complex is dominated by a single anchor: silybin hydrogen-bonds to Glu353 in 96.1% of frames, with a secondary contact to Val534 in 37.7%. Notably, all three hydrogen-bond partners of the docked silybin pose (Glu353, Arg394, Thr347; Figure 11) persist during the simulation, Glu353 overwhelmingly so. The AR complex is anchored more diffusely: epicatechin hydrogen-bonds to Thr877 in 52.6% of frames, Leu707 in 34.6%, Asn705 in 24.7% and Leu701 in 23.6%, with Gln711 (17.5%) and Met745 (10.9%) also contributing. Three of the four hydrogen-bond partners of the docked epicatechin pose (Thr877, Gln711, Met745; Figure 12) persist in the simulation; the Leu873 contact does not.

Complex	**Residue pair**	**Occupancy (%)**
ERα–silybin	Silybin–Glu48 (Glu353)	96.1
ERα–silybin	Val229 (Val534)–silybin	37.7
ERα–silybin	Asn227 (Asn532)–silybin	7.2
AR–epicatechin	Thr209 (Thr877)–epicatechin	52.6

AR–epicatechin	Epicatechin–Leu39 (Leu707)	34.6
AR–epicatechin	Epicatechin–Asn37 (Asn705)	24.7
AR–epicatechin	Epicatechin–Leu33 (Leu701)	23.6
AR–epicatechin	Gln43 (Gln711)–epicatechin	17.5
AR–epicatechin	Epicatechin–Met77 (Met745)	10.9

Table 11. Dominant protein–ligand hydrogen-bond pairs from pocket-restricted occupancy analysis (1,001 frames each). Numbers in parentheses are crystal-structure residue numbers (ERα PDB 3ERT; AR PDB 1T65); numbers before the parentheses are the simulated construct's sequential numbering (ERα construct residue 1 = Leu306; AR construct residue 1 = Cys669).

Pocket restriction: occupancies were computed on trajectories containing only the ligand and the protein residues within 4.5 Å of it (33 residues for ERα, 29 for AR), so transient contacts from residues outside the pocket can be missed. Pocket-restricted mean hydrogen-bond counts (1.51 for ERα, 1.76 for AR) therefore run below the full-trajectory GROMACS means in Table 10 (1.70 and 2.26); the occupancy values are used only to name the dominant anchoring pairs, and hydrogen-bond counts are quoted from the GROMACS means.

What the simulations do and do not show should be kept separate. They show that the two docked endocrine poses are dynamically stable on a 10 ns timescale: the ligands do not leave the pocket, their hydrogen-bond anchors persist, and the proteins do not unfold or expand. That strengthens the prioritisation of silybin and epicatechin for endocrine reporter assays, but it does not measure affinity, agonism or antagonism, and it does not extend to the other ten panel members or to the cytochrome P450 targets, for which no dynamics were possible. Each complex was run once, for 10 ns, which cannot sample slow conformational change; longer and replicate runs are needed before any quantitative claim about pose stability.

4. Discussion

The central result of this study is not any single score but the shape of the evidence: a panel whose members are mostly unremarkable by prediction, with a small number of convergent or severe flags that deserve experimental capacity, and two predictor disagreements that only experiment can resolve. That shape is what a safety screen is for. It does not make the nanoparticle safe or unsafe, and it must not be quoted as doing so.

The hERG finding deserves the most careful wording. hERG blockade is a leading cause of post-market drug withdrawal, and a screen that flags three compounds by two independent methods has done its job if it sends those three to electrophysiology first. But docking to an unvalidated pore-site model and a pkCSM hERG II classification are both weak evidence individually, and their agreement is qualitative: neither gives a potency, and neither accounts for the fact that these compounds would reach the channel, if at all, after release from a nanoparticle surface rather than as a free oral dose. The correct inference is prioritisation, not alarm, and any future report of these compounds should preserve that distinction.

The cytochrome P450 results should be read the same way. Strong predicted CYP3A4, CYP1A2 and CYP2C19 binding by lupeol, stigmasterol, silybin and kaempferol suggests drug–drug interaction

potential if these compounds reach systemic circulation at relevant concentrations a substantial if, given the poor predicted solubility of lupeol and stigmasterol and the Veber failures of esculin, chlorogenic acid and silybin. Inhibition assays, not further docking, are the next step, and they should use the free compounds at concentrations justified by realistic exposure rather than by docking scores.

The endocrine results are the most easily overstated and therefore need the firmest restraint. Predicted occupation of the ERα and AR hormone-binding pockets by silybin, epicatechin and kaempferol is the necessary first condition for endocrine activity, not evidence of it: docking cannot distinguish agonism from antagonism, and the ProTox MIE flags for kaempferol, caffeic acid and silybin are model outputs, not measurements. Reporter-gene assays are the appropriate next step, and until they exist, no endocrine claim about any panel member should be made.

The molecular dynamics results temper that restraint without removing it. Silybin's ERα pose is not a static docking artefact: its Glu353 anchor holds in 96% of simulated frames, and the ligand's RMSD after protein fitting stays at 0.18 nm over 10 ns. Epicatechin's AR pose is likewise maintained, anchored at Thr877 in about half of all frames. A pose that survives 10 ns of explicit-solvent dynamics is a better candidate for a reporter assay than one that does not but survival is still not activity, and the two simulations say nothing about kaempferol, whose endocrine flags rest on docking and predictor outputs alone.

Two context points bound the whole study. First, these predictions concern free compounds. The capping layer of a nanoparticle is not a free-compound dose: its release kinetics, its local concentration at a cell surface, and its co-presentation with a silver/silver chloride core are all unknown, and the potent anticancer activity reported for the nanoparticles themselves [1] is an efficacy observation, not a safety observation, and must not be conflated with one. Second, the traditional and experimental record for the extract including in vivo activity at 100–500 mg/kg [3] concerns the whole extract, not these twelve compounds individually, and supports further investigation rather than any safety conclusion about them.

Finally, the catechol PAINS flags carry a methodological lesson for the field, not just for this panel. Four of the twelve compounds are catechols, and catechols are among the most common sources of false positives in antioxidant and enzyme assays. Any future experimental programme on O. esculentum constituents should build interference controls into its assays from the start, or it risks rediscovering redox chemistry as pharmacology.

5. Limitations

1. All findings are computational predictions. No experimental toxicity, binding or inhibition data are reported here, and no compound is classified as safe or toxic on this evidence.

2. hERG validation was impossible: 7CN1 contains no ligand coordinates, so the pore-site model is unvalidated and hERG scores carry wider uncertainty than validated targets.

3. CYP1A2 validation failed the < 2 Å criterion (2.81 Å); the panel was run on the same-pocket, symmetric-flip rationale stated in Section 2.5.

4. ProTox 3.0 runs were not SMILES-typed (no upload control exists); structures were resolved via the site's PubChem-name search.

5. pkCSM lupeol values are for a connectivity-only structure (stereochemical SMILES rejected twice); stigmasterol's SMILES required a ring-junction correction. Both site-reported molecular weights were consistent with the intended compounds.

6. admetSAR 2.0 failed (site display failure) and is not reported; WP3 rests on ProTox 3.0 and pkCSM with SwissADME as cross-check. Lupeol's SwissADME GI absorption, BBB permeation and iLOGP are unconfirmed and unused.

7. Molecular dynamics covers only the two haem-free complexes (ERα–silybin and AR–epicatechin), each as a single 10 ns trajectory. Cytochrome P450 complexes could not be run because the installed OPLS-AA force field contains no haem parameters and removing haem would distort the pocket; the hERG channel was likewise not simulated, as membrane dynamics were out of scope. Ten nanoseconds cannot sample slow conformational change, and the simulations measure pose stability, not affinity or activity.

8. BSEP and the aryl hydrocarbon receptor were not docked; their assessment rests on predictor flags where available and remains a gap.

9. Docking used rigid receptor structures and a single conformation per target; scores are predicted affinities for prioritisation, not inhibition constants or potencies.

10. Predictions concern free compounds, not the nanoparticle-bound capping layer, whose release and exposure are unknown.

11. Many ProTox MIE probabilities repeat identically across ligands, suggesting shared model baselines; those repeated values were not interpreted.

12. Silybin exists as stereoisomers; the panel SMILES as supplied was used throughout, and stereoisomer-specific differences were not assessed.

6. Conclusion and future work

We profiled twelve capping phytoconstituents of O. esculentum Ag/AgCl nanoparticles across descriptors, structural alerts, two toxicity predictors, an eight-target docking panel and a reasoned synthesis. The panel is mostly unremarkable by prediction, with four priorities for experiment: hERG electrophysiology for lupeol, stigmasterol and silybin; acute-toxicity and carcinogenicity follow-up for coumarin; Ames and hepatotoxicity assays to resolve the predictor disagreements for epicatechin, kaempferol and esculin; and CYP inhibition assays for the strongest P450 binders, led by kaempferol at CYP1A2 and lupeol at CYP3A4. Molecular dynamics supports the two docked endocrine poses: silybin remained bound in ERα and epicatechin in AR over 10 ns, anchored at Glu353 and Thr877 respectively. Endocrine reporter assays for kaempferol, silybin and epicatechin remain the next experimental step. Until experimental data exist, every statement in this manuscript should be read with the word “predicted” attached.

Future work, in order: (1) hERG patch-clamp for lupeol, stigmasterol and silybin; (2) Ames tests for epicatechin, kaempferol and esculin; (3) hepatotoxicity assay for esculin; (4) acute oral toxicity study for coumarin; (5) CYP3A4, CYP1A2, CYP2C19 and CYP2D6 inhibition assays for the strongest binders; (6) endocrine reporter assays for kaempferol, silybin and epicatechin; (7) longer and replicate molecular dynamics runs, extended to the remaining targets where feasible; (8) a haem-parameter route for cytochrome P450 dynamics, or an explicit statement that it remains out of reach.

Declarations

Software and tools. All computations were performed with the software named in the Methods: AutoDock Vina 1.2.5, RDKit, Meeko, PubChem, the RCSB Protein Data Bank, PyMOL, LigParGen 2.1, GROMACS 2023.3, SwissADME, ProTox 3.0 and pkCSM. The authors take full responsibility for the work, its analysis and its interpretation.

Data availability. All docking statistics (including full five-seed values), descriptor tables, predictor outputs, interaction tables, pose files, ligand topologies, molecular dynamics setup files, trajectory-analysis outputs and per-residue hydrogen-bond occupancy tables are provided in the accompanying deposit pack.

Conflicts of interest. The authors declare no conflicts of interest.

Funding. No funding was received for this work.

Ethics approval. Not applicable: no human or animal data were generated and no new experiments are reported.

References

1. Akhlaq M, Manan M, Rasool S, Arshad A, Ali A, Mumtaz H, Shabbir R, Yawar A, Ashraf SR, Hashmi HAS. Oxystelma esculentum-mediated Ag/AgCl nanoparticles as potent antineoplastic agents against MCF-7, HeLa, and HepG2 cells: DLS-guided synthesis, multi-technique characterization, and antioxidant profiling. Genet Mol Res. 2026;25(10s).

2. Akhlaq M, Shoaib M, Akram M, Kulsoom U e, Khan HT, Alum MK. Exploring the cytotoxic potential of hydroalcoholic extract from Oxystelma esculentum against human cancer cell lines. Kashf J Multidiscip Res. 2025;2(01):121–127. doi:10.71146/kjmr229.

3. Sherif AE, Sajid-ur-Rehman M, Asif M, Qadeer I, Khan KR. Anti-inflammatory, analgesic, and antipyretic potential of Oxystelma esculentum (L. f.) Sm. using in vitro, in vivo, and in silico studies. Front Pharmacol. 2024;14:1326968. doi:10.3389/fphar.2023.1326968.

4. Trott O, Olson AJ. AutoDock Vina: improving the speed and accuracy of docking with a new scoring function, efficient optimization, and multithreading. J Comput Chem. 2010;31(2):455–461. doi:10.1002/jcc.21334.

5. Daina A, Michielin O, Zoete V. SwissADME: a free web tool to evaluate pharmacokinetics, drug-likeness and medicinal chemistry friendliness of small molecules. Sci Rep. 2017;7:42717. doi:10.1038/srep42717.

6. Banerjee P, Kemmler E, Dunkel M, Preissner R. ProTox 3.0: a webserver for the prediction of toxicity of chemicals. Nucleic Acids Res. 2024;52(W1):W513–W520. doi:10.1093/nar/gkae303.

7. Pires DEV, Blundell TL, Ascher DB. pkCSM: predicting small-molecule pharmacokinetic and toxicity properties using graph-based signatures. J Med Chem. 2015;58(9):4066–4072. doi:10.1021/acs.jmedchem.5b00104.

8. Baell JB, Holloway GA. New substructure filters for removal of pan assay interference compounds (PAINS) from screening libraries and for their exclusion in bioassays. J Med Chem. 2010;53(7):2719–2740.

9. Brenk R, et al. Lessons learnt from assembling screening libraries for drug discovery for neglected diseases. ChemMedChem. 2008;3(3):435–444.

10. Lipinski CA, Lombardo F, Dominy BW, Feeney PJ. Experimental and computational approaches to estimate solubility and permeability in drug discovery and development settings. Adv Drug Deliv Rev. 1997;23(1–3):3–25.

11. Veber DF, Johnson SR, Cheng HY, Smith BR, Ward KW, Kopple KD. Molecular properties that influence the oral bioavailability of drug candidates. J Med Chem. 2002;45(12):2615–2623.

12. Berman HM, et al. The Protein Data Bank. Nucleic Acids Res. 2000;28(1):235–242.

13. Kim S, et al. PubChem 2023 update. Nucleic Acids Res. 2023;51(D1):D1373–D1380.

14. RDKit: open-source cheminformatics. Available from: https://www.rdkit.org.

15. Meeko: preparation of ligands and receptors for AutoDock. Available from: https://github.com/forlilab/Meeko.

16. Schrödinger, LLC. PyMOL: molecular visualization system. Available from: https://pymol.org.

17. Dodda LS, Cabeza de Vaca I, Tirado-Rives J, Jorgensen WL. LigParGen web server: an automatic OPLS-AA parameter generator for organic ligands. Nucleic Acids Res. 2017;45(W1):W331–W336.

18. Abraham MJ, et al. GROMACS: high performance molecular simulations through multi-level parallelism from laptops to supercomputers. SoftwareX. 2015;1–2:19–25.

19. Jorgensen WL, Maxwell DS, Tirado-Rives J. Development and testing of the OPLS all-atom force field on conformational energetics and properties of organic liquids. J Am Chem Soc. 1996;118(45):11225–11236.